Microstructures and tensile properties of a high strength β titanium alloy Ti5Al4Zr8Mo7V by near β forging and β-transus forging

Wenguang Zhu [a], Jia Lei [a], Qiaoyan Sun [a,*] Lin Xiao[a], Jun Sun [a]

[a] *State Key Laboratory for Mechanical Behavior of Materials, Xi'an Jiaotong University, Xi'an, Shaanxi, 710049, P. R. China.* e-mail address: qysun@xjtu.edu.cn

Abstract

A novel high-strength metastable *β*-Ti alloy Ti-5Al-4Zr-8Mo-7V has been successfully developed by improved Bo-Md map combined with critical Mo equivalent criteria. Near β forging combined with different heat treatments was introduced to tailor the Bi-modal structure. The alloy exhibits good strength-ductility combination with UTS~1390 MPa and El~10% after solution treated (ST) at 800℃ followed by 570℃ aging. After β-transus forging combined with subsequent heat treatment, an excellent combination of strength UTS~1460MPa and El~10% is achieved which is attributed to the Tri-modal structure consisting of primary α (α_p), sub-micro α rods (α_r) and nano-scale α platelets (α_s). Plastic strain is effectively partitioned in both α_p, α_r and β matrix during deformation, which results in a more homogeneously strain distribution and improved ductility. Nano-scale distribution of α_s effectively block the dislocation motion in β matrix and strengthen the alloy.

Keywords: high strength b-Ti alloy; Bo-Md map; microstructure tailoring; tensile property.

1. Introduction

Metastable β titanium alloys are characterized by sufficient β stabilizers such as Mo, V, Ta, Nb, W, Cr, Mn and Fe to ensure retention of β (BCC) phase during rapid cooling to room temperature. Compared to α+β alloys, metastable β-Ti alloys exhibit a combination of high strength-to-weight ratio, reasonable ductility and fracture toughness, which possess an improving share of market for aerospace applications [1, 2]. Recently, there has been a growing interest in design and development of novel β-Ti alloys such as β-CEZ, Ti-5553, Timet-18 and Ti-6554 [3-5].

Control of *α*-phase size, morphology and distribution are of fundamental importance in tailoring mechanical properties of *β*-Ti alloys. Bi-modal structure which consists of equiaxed primary α-phase (α_p) and fine secondary α platelets (α_s) displays an improved strength-ductility combination and fatigue strength [5, 6]. Generally, α_p is the soft phase which sustains more plastic strain during deformation [7-9]. Once the alloy is aged, large amounts of finer α platelets (α_s) are nucleated, which could effectively strengthen the alloy [5, 10, 11]. When the alloy is aged to high strength level, higher strength difference between the soft α_p and aged β matrix will cause local strain incompatibility. Early crack mainly nucleates along a_p/b interface, which will induce tensile instability of the alloy [2, 10]. Thus, modulation of the Bi-modal structure is needed to acquire an improved strength-ductility combination. Many efforts have been made to study the effect of microstructure parameters on the resultant mechanical properties [12-15]. As a novel high strength metastable β alloy Ti-5Al-4Zr-8Mo-7V, effect of both forging process and the following heat treatment on microstructure and the corresponding mechanical properties is still unknown. Under such a requirement, near β forging and β transus forging with different heat treatments were carried out to tailor the microstructure and optimize the strength-ductility combination of this novel Ti-5Al-4Zr-8Mo-7V alloy.

2. Experimental procedures

Triple vacuum arc re-melting (VAR) was introduced to obtain the Ti-5Al-4Zr-8Mo-7V ingot. Subsequently, the coarse grain effectively breaks down by β forging. Then both near β forging at 790℃ and β transus forging at 850℃ with at least 50% deformation is used to control the α phase morphology. Finally, solution treatment followed by different aging temperatures was conducted to optimize the microstructure further. The β transus temperature (T_β) is ~820℃ and the composition is shown in Table 1. Specimens for microstructure observation were mechanically grinded

on a metallographic sandpaper, electrochemical polished and etched in a Kroll's reagent. For tensile property evaluation, ASTM-E8/E8M plate samples (gauge length ~ 25 mm) were prepared and then tested on Instron 1302 testing system.

Table 1 Chemical composition of the novel Ti-5Al-4Zr-8Mo-7V ingot.

Ti	Al	Zr	Mo	V	O	N	H
Bal.	5.04	4.10	7.85	6.88	0.13	0.010	0.004

3. Results and discussion

3.1 Composition determination

An *ab-initio* based model known as the '*d*-electron alloy' design method originally developed by Morinaga has been used to determine the alloy composition [16]. The '*d*-electron theory' provides a physical background to the phase stability which has been successfully applied developing low modulus titanium alloys and TRIP/TWIP alloys [17-20]. In this paper, expansion of this approach to high strength titanium alloy is performed. As is shown in Fig.1, an improved *Bo-Md* diagram based on more than sixty commercial alloys is plotted to determine the composition of high strength β titanium alloy. For determining the composition of high strength β alloys, three rules are used based on this *Bo-Md* diagram. First, the composition of the alloy should locate slightly upper along the β/α+β alloy boundary to obtain high strength. Second, by considering some typical high strength alloys, such as Ti1023, Ti5553, BT22, Ti-17 and Ti7333 which consisting a blue dotted contour line in Fig. 1, the composition of the alloy should be located inside of these target alloys in order to acquire an enhance mechanical property. Third, design of uncertainty strategy is used which means that the composition is located in the unexploited region of the *Bo-Md* diagram. Finally, a composition of Ti-5%Al-4%Zr-8%Mo-7%V in mass percent with the electronic parameters Md=2.376 and Bo=2.774 was determined.

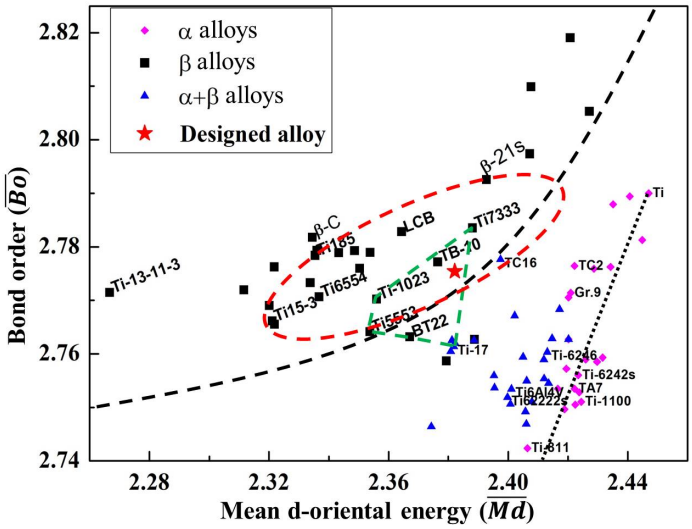

Fig. 1 An improved Bo-Md diagram exhibits the position of designed Ti-5Al-4Zr-8Mo-7V alloy locating both among target alloys and along the β/α+β alloy boundary [9].

3.2 Microstructure and tensile property after near β forging.

Near β forging followed by subsequent heat treatment is traditional process to produce Bi-modal structure. As is clearly seen in Fig.2a, primary α phase (a_p) with globular morphology is homogeneously distributed in β matrix, which is attributed to the dynamic recrystallization of α

phase during near β forging. In addition, owing to the heavy reduction in two phase region, continuous grain boundary a has effectively broken down and transformed into globular shape (see in Fig.2b).

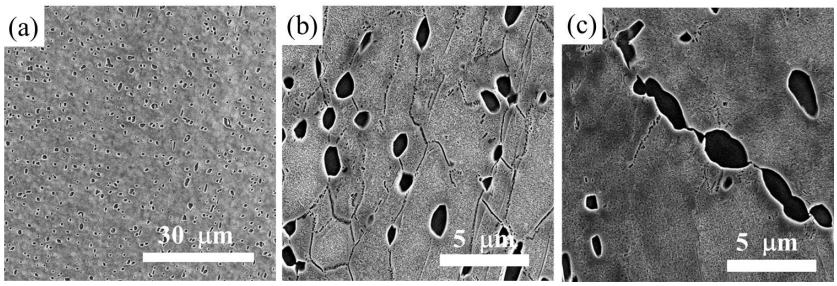

Fig. 2 Microstructure of Ti-5Al-4Zr-8Mo-7V after near β forging: (a) and (b) represent the images of intragranular and grain boundary morphology respectively.

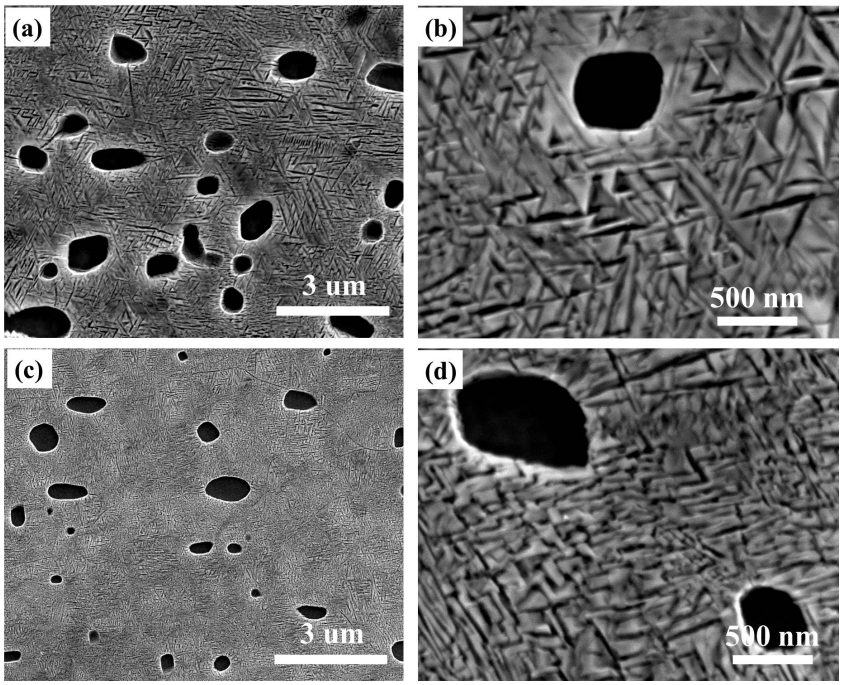

Fig. 3 (a) and (b) represents the microstructure of the alloy solution treated at 780℃ and aged at 510℃ for 6h, (c) and (d) is the alloy solution treated at 810℃ and aged at 510℃ for 6h.

Fig. 3 shows the effect of solution temperature on microstructure evolution of the alloy. As is clearly seen in Fig. 3a and 3c, volume fraction of α_p decreases dramatically with increasing solution temperature and the size of α_s is finer after solution treated at lower temperature. By using the Image-pro Plus software, statistical results of volume fraction of α_p is recorded, which decreases from 7.1% to 3.1% as the ST temperature increasing from 780℃ to 810℃. The decrease of α_p leads to a decrease of b phase stability, which will increase the driving force for α nucleation during aging. Thus high fraction nano-scaled a_s is precipitated after high temperature solution treatment, as seen in Fig.3c and 3d. The tensile

property of the alloy solution treated at 780℃ and 810℃ is shown in Table 2. The strength of the alloy is increasing with elevating temperature. The alloy solution treated at high temperature (810 ℃) followed by low temperature (510 ℃) aging shows an extremely high strength UTS~1632MPa but limited ductility El~6.2%. This is attributed to the high fraction nano-scale α_s which significantly hinders dislocations slip in β matrix. The larger amount of finer α_s, the higher would be the strength.

Table 2 Effect of solution treatment temperature on mechanical properties

STA	UTS/MPa	st.dev.	YS/MPa	st.dev.	El/%	st.dev.
810-510/6h	1632	8.7	1586	9.4	6.3	0.03
780-510/6h	1512	17.2	1442	15.6	6.1	0.23

Fig. 4 shows the effect of aging temperature on microstructure evelotion of the alloy after solution treated at 800℃. Different from large globular primary α phase, precipitation of much finer lamella α phase (α_s) takes place during aging, which obeys the Burgers orientation with β matrix (i.e. $(110)_\beta$ // $(0001)_\alpha$ and $[1\text{-}11]_\beta$ // $[11\text{-}20]_\alpha$) [2]. In general, the size of α_s increases and the fraction decreases with incremental aging temperature. As for aging at low temperature, owing to the large driving force for nucleation and sluggish kinetics for growth, large amouts of nano-scale a_s precipated (see Fig. 4a and b). On the contary, coarse a_s with lower fraction is precipatied during aging at high temperature (see in Fig. 4e and 4f). In additon, it's obviously seen that the size distribution of a_s is inhomogeneous at 600℃ aging. The large coarse a_s region probably yields at low stress and results in strain localization. Owing to the large slip length of β matrix in coarse a_s region, dislocation behaviour is relaxed comparing to small slip length of beta matrix from aging at low tempertature aging, which could result in a decrease in strength.

Fig. 5 shows the tensile properties of the alloy after ST at 800℃ with different aging temperature. The alloy displays a decrease in strength and increase in ductility with incremental aging temperature, which has been reported in many other high strength b titanium alloys [7, 12, 21]. Fig. 5b shows the correlation of the α_s spacing length and the tensile properties. It is seen that an increase of α_s spacing length results in a decrease in strength and increase in ductility. This indicates that spacing length of α_s probably dominates the dislocation behaviour in β phase which in turn determines the strength of the alloy. Detailed tensile property of the alloy with Bi-modal structure after different heat treatments is shown in Table 3. The alloy exhibits extremely high tensile strength (UTS~1512-1632 MPa) but a relatively poor elongation (El~5.1%-6.2%) aging at 510℃. A good combination of strength and ductility is abtained after solution treatment at 800℃ followed by aging at 540℃ and 570℃. High tensile strength (UTS~1390MPa) with prominent elongation (El~10%) is obtained after 570℃ aging.

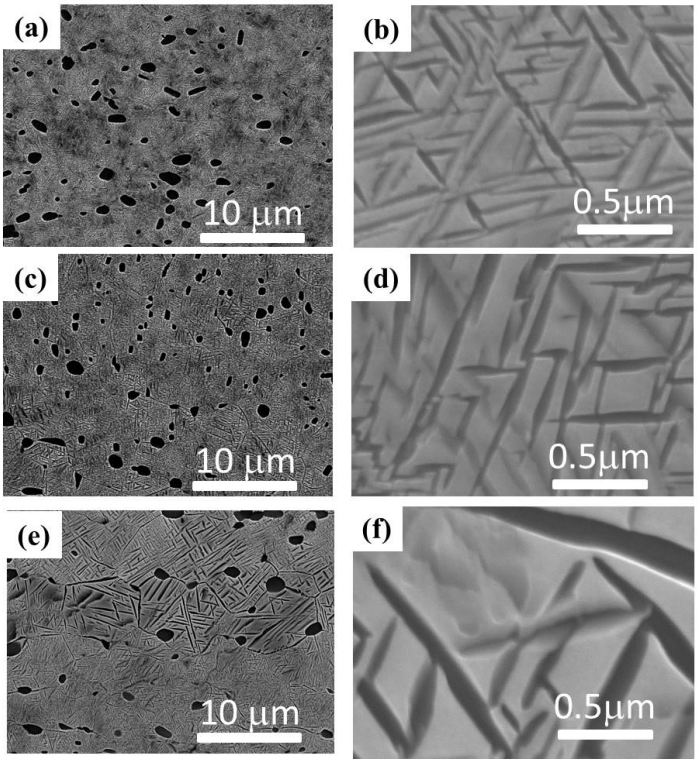

Fig. 4 Influence of aging temperature on microstructure of the alloy solution treated at 800℃: (a), (b) 540℃; (c), (d) 570℃; (e), (f) are 630℃

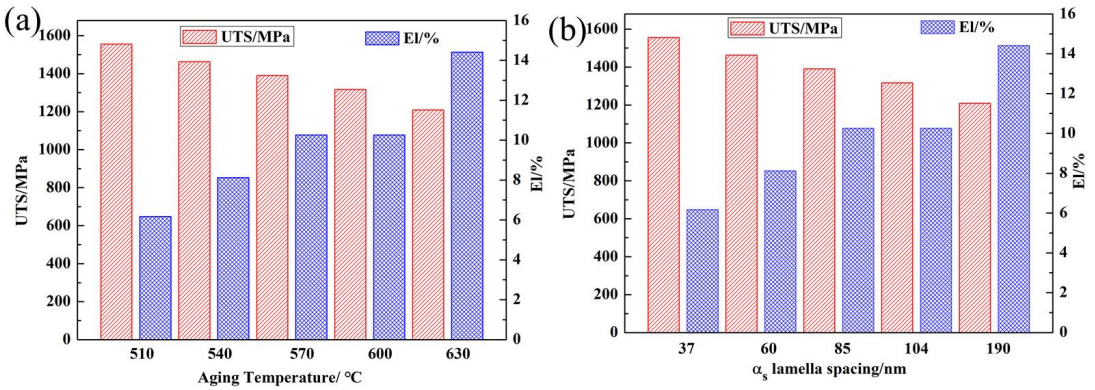

Fig. 5 Influence of aging temperature on tensile property of the alloy ST at 800℃ : (a) represent the effect of aging temperature on tensile property of the alloy, (c) is the corresponding spacing length of α_s lamella versus tensile property. UTS and El are the ultimate tensile strength and elongation at fracture respectively.

3.3 Microstructure and deformation behavior of β transus forged alloy.

Fig. 6 shows the microstructure of the alloy after β transus forging followed by solution treated at 760℃ and 600℃ aging. Owing to the insufficient reduction in α/β two phase region, grain boundary α-phase is in form of necklace-like shape. The intragranular α-precipitates are in three types of morphologies, (i.e. the Tri-modal structure), which is consisted of elongated primary α-phase (α_p), submicron α-rods (α_r) and nano-scaled α-platelets (α_s), as seen in Fig. 6b and 6c.

Fig. 7a presents uniaxial tensile curves of the Tri-modal sample in comparison with Bi-modal structure of equivalent strength (Bi-modal 1) or elongation (Bi-modal 2). It can be seen that Tri-modal structure exhibits high yield strength with large uniform elongation. The ultimate tensile strength was measured to be ~1460 MPa and the elongation at fracture reaches 10%. As is shown in Fig. 7b, tensile properties of the Tri-modal sample are compared with that of other as-reported high-strength β-Ti alloys [1, 7, 10, 12, 22, 23]. It is indicated that via β transus forging and the following heat treatments, the Ti-5Al-4Zr-8Mo-7V alloy exhibits Tri-modal structure which possesses an excellent combination of strength and ductility in comparison to the other high-strength β-Ti alloys such as Ti5553, Ti-1023, Ti-17, BT22 and Ti-7333.

Table 3 Tensile property of the alloy with Bi-modal structure after different heat treatments

(α-β)STA	UTS MPa	YS MPa	El %
780-510/6h	1512	1442	6.1
780-540/6h	**1420**	**1373**	**8.1**
780-570/6h	1303	1269	11.7
780-600/6h	1259	1239	11.4
780-630/6h	1141	1110	13.8
800-510/6h	1555	1526	6.2
800-540/6h	**1463**	**1428**	**8.1**
800-570/6h	**1390**	**1343**	**10.3**
800-600/6h	1317	1279	10.3
800-630/6h	1209	1159	14.4
810-510/6h	**1632**	**1586**	**6.3**
810-540/6h	1446	1388	6.0
810-570/6h	1370	1305	8.3
810-600/3h	1212	1139	15.3

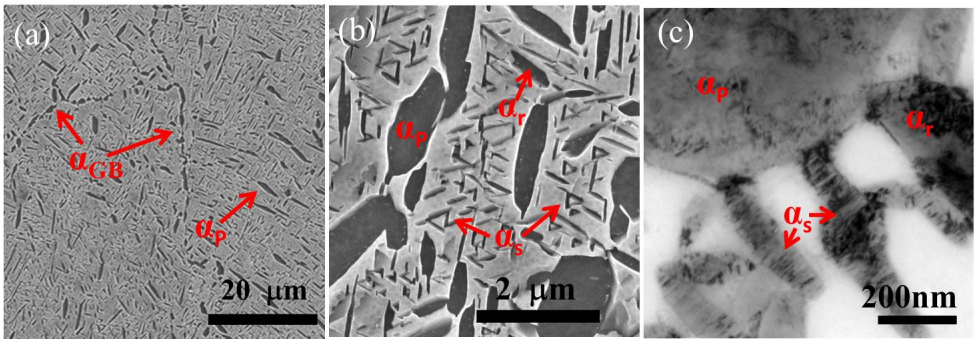

Fig. 6 Microstructure of Tri-modal structure after β transus forging followed by ST at 760℃ and aging at 600℃: (a) SEM image showing the elongated primary α phase (α_p) and the discontinuous grain boundary α phase. (b) the Tri-modal structure consisting of elongated primary α (α_p), submicron α rod (α_r) and nano-scaled α platelets (α_s). (c) TEM image of the Tri-modal structure.

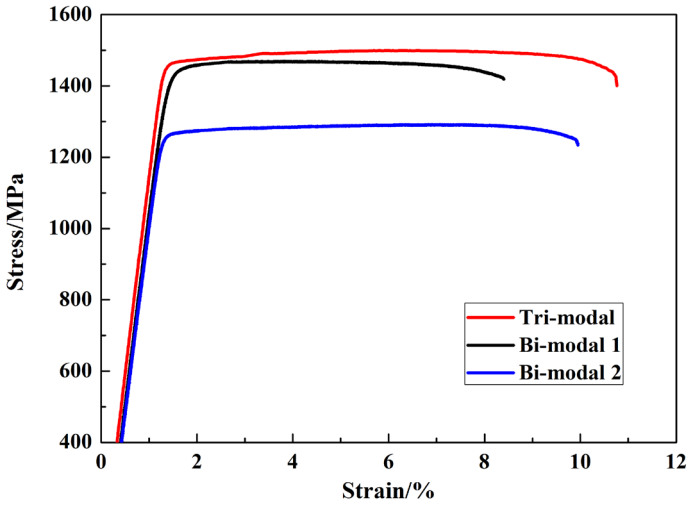

Fig. 7 Tensile property of the alloy with Tri-modal structure: stress-strain curve in comparison with Bi-modal structure of equivalent strength (Bi-modal 1) or elongation (Bi-modal 2)

The plastic deformation behavior of the complex Tri-modal structure is discussed to explain the improved strength-ductility combination. Since the aged samples contain a mixture of a phase with different combinations of size, morphology, and volume fraction, it is very difficult to separate the individual contributions of each factor to plastic deformation. In general, the plastically constrained β/α_s aggregates are considered to be stronger, and slip initiates from the soft a_p phase [2, 24]. Our former TEM observation also demonstrates that high density of GND (geometrical necessity dislocation) accumulated at soft a_p interface which strengthens the a_p during deformation effectively. Then α_p deforms like composite material consisting of dislocation-free phase interiors with lower flow stress and hard grain-boundary layers [25, 26]. During further deformation, the compliant phase interiors of a_p can deform plastically and sustain more strain partition. The hard grain-boundary layer can deform with the submicron α_r and transformed β matrix compatibly. This is evidenced by the TEM observation that large amounts of tangled dislocation is found in both α_r and α_p after tensile [9]. Finally, the plastic strain is partitioned in the α_p, α_r and β_{trans} matrix effectively, which results in a more homogeneous strain gradient and enhanced ductility in the alloy.

4. Conclusions

(1) Via traditional near β forging and the subsequent heat treatment, Bi-modal structure of the alloy is tailored which exhibits a good strength-ductility combination.

(2) Tri-modal microstructure is developed by β transus forging and the subsequent heat treatment, which shows better tensile properties than Bi-modal microstructure.

Acknowledgment

This work was supported by the National Natural Science Foundation of China (Grant No.51671158), the 973 Program of China (2014CB644003).

Reference

[1] S.L. Nyakana, J.C. Fanning, R.R. Boyer, Quick reference guide for β titanium alloys in the 00s, Journal of Materials Engineering and Performance 14(6) (2005) 799-811.

[2] D. Banerjee, J.C. Williams, Perspectives on Titanium Science and Technology, Acta Materialia 61(3) (2013) 844-879.

[3] S. Shekhar, R. Sarkar, S.K. Kar, A. Bhattacharjee, Effect of solution treatment and aging on microstructure and tensile properties of high strength β titanium alloy, Ti–5Al–5V–5Mo–3Cr, Materials & Design 66(Part B) (2015) 596-610.

[4] J. Fan, J. Li, H. Kou, K. Hua, B. Tang, Y. Zhang, Microstructure and mechanical property correlation and property optimization of a near β titanium alloy Ti-7333, Journal of Alloys & Compounds 682 (2016) 517-524.

[5] Z. Du, S. Xiao, L. Xu, J. Tian, F. Kong, Y. Chen, Effect of heat treatment on microstructure and mechanical properties of a new β high strength titanium alloy, Materials & Design 55(55) (2014) 183-190.

[6] J.O. Peters, G. Lütjering, M. Koren, H. Puschnik, R.R. Boyer, Processing, microstructure, and properties of β-CEZ, Materials Science and Engineering: A 213(1) (1996) 71-80.

[7] J. Fan, J. Li, H. Kou, K. Hua, B. Tang, Y. Zhang, Microstructure and mechanical property correlation and property optimization of a near β titanium alloy Ti-7333, Journal of Alloys and Compounds 682 (2016) 517-524.

[8] Y. Wang, M. Chen, F. Zhou, E. Ma, High tensile ductility in a nanostructured metal, Nature 419 (2002) 912.

[9] W. Zhu, J. Lei, C. Tan, Q. Sun, W. Chen, L. Xiao, J. Sun, A novel high-strength β-Ti alloy with hierarchical distribution of α-phase: The superior combination of strength and ductility, Materials & Design 168 (2019) 107640.

[10] G.T. Terlinde, T.W. Duerig, J.C. Williams, Microstructure, tensile deformation, and fracture in aged ti 10V-2Fe-3Al, Metallurgical Transactions A 14(10) (1983) 2101-2115.

[11] C.M. Liu, H.M. Wang, X.J. Tian, H.B. Tang, D. Liu, Microstructure and tensile properties of laser melting deposited Ti–5Al–5Mo–5V–1Cr–1Fe near β titanium alloy, Materials Science and Engineering: A 586 (2013) 323-329.

[12] O.M. Ivasishin, P.E. Markovsky, Y.V. Matviychuk, S.L. Semiatin, C.H. Ward, S. Fox, A comparative study of the mechanical properties of high-strength β-titanium alloys, Journal of Alloys and Compounds 457(1-2) (2008) 296-309.

[13] O.M. Ivasishin, P.E. Markovsky, S.L. Semiatin, C.H. Ward, Aging response of coarse- and fine-grained β titanium alloys, Materials Science and Engineering: A 405(1-2) (2005) 296-305.

[14] C.-L. Li, X.-J. Mi, W.-J. Ye, S.-X. Hui, Y. Yu, W.-Q. Wang, A study on the microstructures and tensile properties of new beta high strength titanium alloy, Journal of Alloys and Compounds 550 (2013) 23-30.

[15] L. Ren, W. Xiao, H. Chang, Y. Zhao, C. Ma, L. Zhou, Microstructural tailoring and mechanical properties of a multi-alloyed near β titanium alloy Ti-5321 with various heat treatment, Materials Science and Engineering: A 711 (2018) 553-561.

[16] M. Abdel-Hady, K. Hinoshita, M. Morinaga, General approach to phase stability and elastic properties of β-type Ti-alloys using electronic parameters, Scripta Materialia 55(5) (2006) 477-480.

[17] M. Abdel-Hady, K. Hinoshita, H. Fuwa, Y. Murata, M. Morinaga, Change in anisotropy of mechanical properties with β-phase stability in high Zr-containing Ti-based alloys, Materials Science & Engineering A 480(1–2) (2008) 167-174.

[18] Y. Abd-elrhman, M.A.H. Gepreel, A. Abdel-Moniem, S. Kobayashi, Compatibility assessment of new V-free low-cost Ti–4.7Mo–4.5Fe alloy for some biomedical applications, Materials & Design 97 (2016) 445-453.

[19] L. Ren, W. Xiao, C. Ma, R. Zheng, L. Zhou, Development of a high strength and high ductility near β-Ti alloy with twinning induced plasticity effect, Scripta Materialia 156 (2018) 47-50.

[20] C. Brozek, F. Sun, P. Vermaut, Y. Millet, A. Lenain, D. Embury, P.J. Jacques, F. Prima, A β-titanium alloy with extra high strain-hardening rate: Design and mechanical properties, Scripta Materialia 114 (2016) 60-64.

[21] O.M. Ivasishin, P.E. Markovsky, Y.V. Matviychuk, S.L. Semiatin, Precipitation and recrystallization behavior of beta titanium alloys during continuous heat treatment, Metallurgical and Materials Transactions A 34(1) (2003) 147-158.

[22] W. Gerhard, R.R. Boyer, E.W. Collings, Materials properties handbook: Titanium alloys, (1994).

[23] J.C. Fanning, Properties of TIMETAL 555 (Ti-5Al-5Mo-5V-3Cr-0.6Fe), Journal of Materials Engineering and Performance 14(6) (2005) 788-791.

[24] D. Lunt, X. Xu, T. Busolo, J. Quinta da Fonseca, M. Preuss, Quantification of strain localisation in a bimodal two-phase titanium alloy, Scripta Materialia 145 (2018) 45-49.

[25] H.H. Fu, D.J. Benson, M.A. Meyers, Analytical and computational description of effect of grain size on yield stress of metals, Acta Materialia 49(13) (2001) 2567-2582.

[26] X.L. Wu, M.X. Yang, F.P. Yuan, L. Chen, Y.T. Zhu, Combining gradient structure and TRIP effect to produce austenite stainless steel with high strength and ductility, Acta Materialia 112 (2016) 337-346.